

Differential Susceptibility to Quantum Dot Induced Lung
Inflammation: A Systems Genetics Approach

David K Scoville

A thesis submitted in partial fulfillment of the
requirements for the degree of Master of Science

University of Washington

2012

Committee:

Terrance J Kavanagh
William C Parks
David L Eaton

Program Authorized to Offer Degree:

Department of Environmental and Occupational Health Sciences – Public Health

University of Washington

Abstract

Differential Susceptibility to Quantum Dot Induced Lung Inflammation:
A Systems Genetics Approach

David K Scoville

Chair of Supervisory Committee:

Professor Terrance J Kavanagh

Department of Environmental and Occupational Health Sciences

Quantum dots (QDs) are nanoparticles typically composed of a CdSe core, a ZnS shell, and an assortment of polymer coatings specific to their application. Unique fluorescent properties of QDs make them useful in biomedical imaging. However, due to their small size and heavy metal composition, there is concern over the possible toxicity of QDs. We have examined 8 genetically inbred parental mouse strains from the Collaborative Cross (CC) for their differential susceptibility to QD-induced lung inflammation using % neutrophils and total protein in bronchoalveolar lavage fluid (BALF) as inflammation biomarkers. Oropharyngeal aspiration was used to deliver a 6 ug Cd equivalents/kg BW dose of QDs into the lungs of the different strains of mice. Flow cytometry and the Bradford Assay were used to measure the % neutrophils and total protein in BALF, respectively. In an attempt to explore whether mechanisms that are currently thought to mediate QD toxicity seem to be playing a role in these mice, Cd and total GSH levels were measured in lung tissue using ICP-MS, and derivatization with naphthalene-2,3-dicarboxaldehyde (NDA) with fluorescence detection, respectively. Significant variation was observed in biomarkers of QD induced inflammation, due to both QD treatment and genetic differences among mouse strains. In our exploration of Cd and GSH, an interaction was observed between GSH and the % neutrophils in BALF. Inverse correlations were seen between mean GSH levels and % neutrophils in BALF in

all treatment groups. We also observed that Cd levels positively correlated with the % of neutrophils in BALF, and that GSH and Cd are inversely correlated, possibly indicating that QDs are releasing Cd, depleting GSH and resulting in oxidative stress. Future studies using recombinant inbred or Diversity Outcross strains created from the Collaborative Cross will be used to map potential quantitative trait loci (QTLs) associated with QD-induced lung inflammation and oxidative stress. Analysis of such QTLs could lead to insights regarding the molecular mechanisms responsible for QD toxicity and ultimately provide guidance to manufacturers on how to produce safer QDs.

TABLE OF CONTENTS

	Page
List of Figures	ii
List of Tables	iii
1. Introduction.....	1
2. Materials and Methods.....	5
2.1. Animals	5
2.2. Quantum Dots	7
2.3. Oropharyngeal Aspiration of QDs	8
2.4. Bronchalveolar Lavage	8
2.5. Cytospin and Flow Cytometry	8
2.6. Cadmium Analysis	9
2.7. Total Protein.....	9
2.8. Total Glutathione	10
2.9. Data Analysis / Statistical Methods	10
3. Results.....	11
3.1. Neutrophils in BALF.....	12
3.2. Total Protein in BALF	13
3.3. Cadmium in Lung Tissue.....	14
3.4. Total GSH in Lung Tissue	16
3.5. Glutathione and Cadmium Correlation	17
4. Discussion.....	18
References.....	25

LIST OF FIGURES

Figure Number	Page
Figure 1. Quantum Dots.....	7
Figure 2. % Neutrophils in BALF.....	11
Figure 3. Total Protein in BALF.....	13
Figure 4. Cadmium Content in Right Lung Tissue	14
Figure 5. Total Glutathione in Right Lung Tissue	15
Figure 6. Glutathione and Cadmium Correlation	17

LIST OF TABLES

Table Number	Page
Table 1. Body Weights and Doses	5

1. Introduction

Nanoparticles are characterized as objects where at least one dimension of the object is in the 1-100 nm size range ([Iavicoli et al. \(2010\)](#)). Quantum Dots (QDs) are a type of nanoparticle with a semiconductor crystalline core that can consist of CdSe or other heavy metals. A ZnS shell, with an optimal number of layers (≤ 3) to balance increasing stability while maintaining maximum quantum yield, is added to the core to balance fluorescence emission and durability in acidic conditions ([Medintz et al. 2005](#); [Hoshino et al. 2011](#)). The fluorescent properties of QDs vary with size such that the emission spectrum ranges from approximately 400 nm, which is in the violet range, to 1,350 nm, which is in the near infrared range, depending on whether the QD core is 2 or 10 nm diameter, respectively. In addition to the core and shell composition, QDs have outer coatings that affect their fluorescence as well as their other physicochemical and biological properties ([Hoshino et al. 2011](#)). The diversity of outer coatings for QDs is what provides the potential for a variety of uses.

Some of the biomedical applications for QDs are improved drug delivery and targeted cell imaging. QDs are especially well suited for cell labeling because of their superior quantum yield and increased resistance to photobleaching compared to traditional organic dyes and fluorophores ([Hoshino et al. 2011](#)). It has been shown that doxorubicin conjugated QDs can be taken into to the nucleus of alveolar macrophages, effectively killing the cells with minimal residual damage and relatively little inflammation ([Chakravarthy et al. 2011](#)). Nuclear targeting in non-phagocytic HeLa cells has also been achieved ([Chen and Gerion 2004](#)). This is significant because images from a study looking at co-localization of QDs with mitochondria and lysosomes did not show

many QDs in the area of the cell assumed to be the nucleus ([Clift et al. 2011](#)) and entry into the nucleus is necessary for drugs that target DNA synthesis. There has also been success using QDs to selectively label cell surface markers, including Her2 in breast cancer cells, with monoclonal antibody conjugated QDs ([Wu et al. 2003](#)), as well as to identify and deliver doxorubicin to mutated mucin-1 expressing multidrug resistant A2780/AD ovarian carcinoma cells using dual conjugated QDs ([Savla et al. 2011](#)). Another use of QDs is *in vivo* imaging of cancerous cells in tumors and other tissues ([Savla et al. 2011](#)). One study successfully used QDs to label sentinel lymph nodes in mice, which could improve current lymph node imaging and provide for more efficient surgical removal of involved tissue ([Kim et al. 2004](#)). All of these studies demonstrate the potential value of QDs in medical diagnostics and treatment. Other uses include phototonics (e.g. solar panels, LED lighting), specialty paints and dyestuffs, molecular tracers, and signal detection systems.

It is precisely because of the widespread utility of QDs and their proposed uses in medicine and science that their toxic effects need to be fully understood. Numerous *in vitro* studies have indicated that QDs can exhibit cytotoxicity ([Shiohara et al. 2004](#); [Kirchner et al. 2005](#); [Lovric et al. 2005](#); [Lovrić et al. 2005](#); [Zhang et al. 2008](#); [Clift et al. 2010](#); [Yazdi et al. 2010](#); [McConnachie et al. 2012](#)). However, relatively few *in vivo* toxicity studies have been performed and most have found little toxicity following intravenous (iv) administration of QDs ([Hauck et al. 2010](#); [Su et al. 2011](#); [Ye et al. 2012](#)). However, one study performed in mice found that QDs given through iv injection lead to formation of multiple thrombi that contained QDs that were found in the lungs, but were avoided in other experiments where mice were pretreated with heparin ([Geys et](#)

[al. 2008](#)). A mechanism of toxicity proposed for QDs is through generation of reactive oxygen species and subsequent ‘oxidative stress’ ([Lovrić et al. 2005](#); [Clift et al. 2010](#)). This seems feasible since QDs can release Cd ions ([Derfus et al. 2004](#); [Kirchner et al. 2005](#); [Su et al. 2010](#)) and Cd can cause oxidative stress ([Watanabe et al. 2003](#)) via generating reactive oxygen species (ROS) by disrupting the electron transport chain ([Wang et al. 2004](#)). The cytotoxicity seen by Lovric et al (2005) was attenuated by N-acetyl-cysteine (NAC), indicating the potential for the involvement of reduced glutathione (GSH) since NAC can support GSH synthesis. In fact, GSH levels were depleted after treatment of a macrophage cell line with QDs ([Clift et al. 2010](#)). It has also been shown that QD outer coatings may contribute to the intrinsic toxicity of QDs ([Hoshino et al. 2004](#)). Inflammation has also been reported with QD exposure. Macrophages play a large role in the inflammatory response through the secretion of proinflammatory cytokines resulting in the recruitment of neutrophils and other inflammatory cells, as well increased vascular permeability to accommodate cellular influx. QDs are taken up by macrophages ([Hoshino et al. 2009](#)) via phagocytosis and macropinocytosis if serum is present and there is aggregation, and by clathrin and caveolin mediated endocytosis for non aggregated QD-conjugates ([Chakravarthy et al. 2011](#)). The involvement of the immune system complicates the toxicity of QDs considerably and also warrants exploration of their effects *in vivo*. Immune effects of QDs have been studied *in vitro and in vivo* ([Hoshino et al. 2009](#)). Several studies found that QDs cause pulmonary inflammation after intratracheal instillation ([Jacobsen et al. 2009](#)), and inhalation ([Ma-Hock et al. 2012](#)). In other studies, polynucleotide conjugates attached to the QDs (but not the QDs themselves) were implicated in the inflammatory

response ([Hoshino et al. 2009](#)). However, data from our lab, supported by other modeling studies ([Jacobsen et al. 2009](#)) and direct inhalation studies ([Ma-Hock et al. 2012](#)), suggest that when introduced to the lungs, QDs can cause inflammation independent of the formation of polynucleotide conjugates. Inhalation of aerosolized QDs, followed by deposition in the lung, is a plausible route of occupational exposure, given the size of QDs and their potential to aerosolize. In the current study we used oropharyngeal aspiration to deliver QDs to the lungs of multiple strains of mice.

The Collaborative Cross is an international effort to use genetically diverse inbred parental strains of mice to develop new recombinant inbred strains so as to better map genes, and to model genetic diversity in the human population ([Churchill et al. 2004](#)). In this project we used the 8 parental strains from the Collaborative Cross which included 5 inbred laboratory strains of mice (C57BL/6J, 129X1/SvJ, A/J, NOD/LtJ, and NZO/HILtJ) and 3 wild derived strains (CAST/EiJ, PWK/PhJ, and WSB/EiJ). The goal was to use a systems genetics approach for exploring and mapping genes associated with QD-induced lung inflammation and oxidative stress. Systems genetics focuses on using technologies such as genomics, proteomics, metabolomics and DNA sequencing to investigate the relationships between genetic information and whole organism function ([Nadeau and Dudley 2011](#)). Recently, a study using the 8 parental strains and 131 incipient recombinant inbred strains from the Collaborative Cross successfully mapped QTLs for hematologic parameters, including red blood cell volume, white blood cell count, percent neutrophils and macrophages, and monocyte number ([Kelada et al. 2012](#)).

In summary, the main objectives of this study were to establish whether QDs induced an inflammatory response when delivered to the lungs via oropharyngeal

aspiration, and whether this response differed among the 8 parental Collaborative Cross inbred mouse strains. In addition, Cd and GSH were measured in lung tissue to determine if the presence of either QDs or released Cd ions was associated with oxidative stress in these mice.

Strain	Treatment Group	Body Weight (g)	(95%CI)	Dose (ul)	(95% CI)
129	Sal	23.08	(21.2 - 24.97)	35.33	(32.55 - 38.11)
	QD	22.67	(21.13 - 24.21)	33.92	(30.83 - 37)
AJ	Sal	21.5	(19.91 - 23.09)	32.83	(30.4 - 35.26)
	QD	22.6	(20.72 - 24.48)	34.6	(31.48 - 37.72)
B6	Sal	25.33	(23.94 - 26.72)	38.75	(36.58 - 40.92)
	QD	25.08	(23.98 - 26.18)	38.33	(36.57 - 40.1)
CAST	Sal	15.2	(14.16 - 16.24)	23	(21.48 - 24.52)
	QD	14.83	(14.4 - 15.26)	22.67	(21.81 - 23.52)
NOD	Sal	23.83	(22.03 - 25.64)	36.4	(32.93 - 39.87)
	QD	41.2	(37.14 - 45.26)	35	(31.96 - 38.04)
NZO	Sal	39.33	(38.06 - 40.6)	60.17	(58.13 - 62.2)
	QD	16.67	(14.83 - 18.5)	63	(56.92 - 69.08)
PWK	Sal	17.17	(15.36 - 18.97)	26.33	(23.32 - 29.35)
	QD	16.67	(14.83 - 18.5)	25.33	(22.24 - 28.42)
WSB	Sal	16.5	(15.4 - 17.6)	25.17	(23.24 - 27.09)
	QD	15.5	(14.93 - 16.07)	23.5	(22.93 - 24.07)

Table 1. Body Weights and Doses. The mean and 95% CI of the mean body weight (g) and dose (ul) received for each strain and treatment group. Note that body weight was not measured for untreated animals.

2. Materials and Methods

2.1. Animals

All mice were purchased from Jackson Laboratories (Bar Harbor, ME) and shipped around 6 weeks of age. Twelve 129X1/SvJ, CAST/EiJ A/J, NOD/LtJ, NZO/HILtJ, PWK/PhJ, and WSB/EiJ were ordered. Since C57BL/6J is the most common laboratory mouse and data for similar projects exists for this strain, it served as a reference strain for evaluating the experimental procedure. Supplemental orders of

129X1/SvJ and CAST/EiJ were made to address questions of variability. To obtain baseline measures (i.e. no treatment), 4 additional mice of each of the 8 strains were ordered. All experiments were done within 4-weeks of arrival of the mice in the vivarium. Animals were housed in a modified Specific Pathogen Free facility at the University of Washington. All experiments and methods were approved by the University of Washington Institutional Animal Care and Use Committee (IACUC).

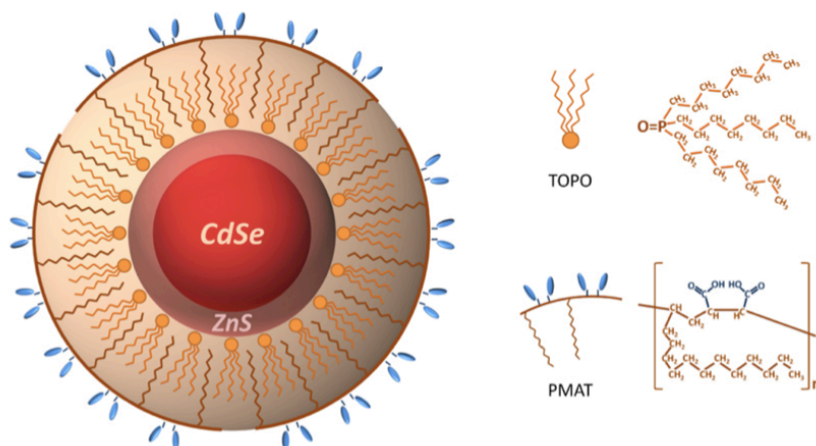
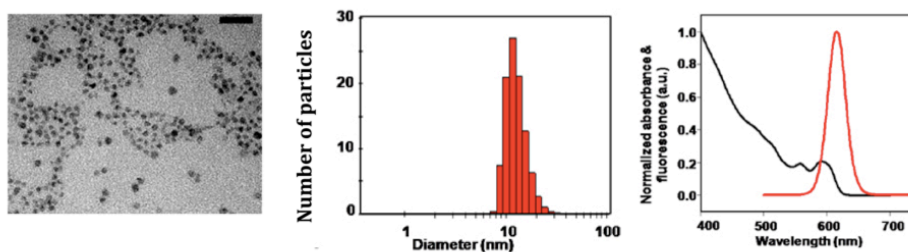
A**B**

Figure 1. Quantum Dots (A) Diagram of quantum dots used in this study. The QD has a Cd/Se core, is surrounded by a Zn/S shell, and has a TOPO-PMAT coating. (B) From left to right: An electron micrograph of TOPO-PMAT QDs, a histogram of the size distribution of the QDs, and a plot of the excitation/emission spectra for the QDs. (modified from McConnachie et al., 2012)

2.2. Quantum Dots

The QDs in our study were generously provided to us by Dr. Xiaohu Gao in the Department of Bioengineering at the University of Washington. They consist of a Cd/Se core, a Zn/S shell, and an outer amphiphilic polymer coating of trioctylphosphine oxide

(TOPO), poly (maleic anhydride-alt-1- tetradecene) (PMAT). They were approximately 12 nm in hydrodynamic diameter, and had a peak fluorescence emission at 620 nm.

2.3. Oropharyngeal Aspiration of QDs

Animals were anesthetized prior to treatment using an anesthesia machine from Summit Anesthesia Solutions with a 2L/min oxygen flow with 4% Isoflurane. Mice received a dose of TOPO-PMAT CdSe/ZnS QDs equivalent to 6 ug Cd/kg Body Weight (BW), given as a 10 nM saline solution (0.9% NaCl) via oropharyngeal aspiration (OPA). The calculation of the dose of 6 ug/kg BW cadmium equivalent from a 10 nm solution of QDs was based on the assumption that there are approximately 3500 atoms of cadmium per QD. Control animals received 1.53 ul 0.9% saline/g BW via OPA. Four animals from each strain received no treatment.

2.4. Bronchoalveolar Lavage

Eight hr after dosing, mice were euthanized and bronchoalveolar lavages (BAL) were performed 3 times with 3 triturations of 1 mL phosphate buffered saline (PBS) per lavage, as previously described ([Weldy et al. 2011](#)), with the exception of CAST/EiJ, WSB/EiJ, and PWK/PhJ mice which received 700 uL PBS due to the reduced lung volume in these smaller strains.

2.5. Cytospin and Flow Cytometry

Fifty uL of BALF from the 1st lavage was diluted with 450 mL of RT PBS and then added to a Shandon Cytospin cartridge (ThermoScientific, Waltham, MA). The

cartridges were centrifuged at 600 rpm for 10 minutes and the deposited cells were stained using Diff-Quik Fixative (Siemens Healthcare Diagnostics, Newark, DE) for cell differential counts. The remaining BALF was centrifuged, the 1st lavage supernatant was stored at -80° C for later analysis, and the 2nd and 3rd lavage supernatant was discarded. The cells from all lavages were pooled and processed for immunohistochemical staining for macrophages and neutrophils ([Weldy et al. 2011](#)).

2.6. Cadmium Analysis

Samples were taken from frozen tissues, weighed and put into nitric acid/heat resistant vials. Cadmium content in tissues and serum was determined by Inductively Coupled Plasma Mass Spectrometry (ICP-MS) following modified EPA Method 6020A ([EPA 2007](#)) with an Agilent 7500ce ICP-MS by the University of Washington Environmental Health Laboratories and Trace Organics Analysis Center.

2.7. Total Protein

Total protein in the BALF was measured using the Bio-Rad Protein Assay (BioRad, Hercules, CA) . A standard curve with known amounts of protein (bovine serum albumin) was created (0-0.35mg/ml). Ten uL of BALF and 200 ul of dye reagent were added to a 96-well plate in triplicate. The absorbance at 590 nm was measured using a SpectraMax 190 plate reader (Molecular Devices, Sunnyvale, CA) after a 10 min incubation.

2.8. Total Glutathione

Total glutathione levels in lung homogenate was measured by reducing all glutathione to GSH using tris(2-carboxyethyl)phosphine (TCEP) and derivatizing with naphthalene-2,3-dicarboxaldehyde (NDA) ([Weldy et al. 2011](#)).

2.9. Data Analysis / Statistical Methods

All data were processed and analyzed using either Microsoft Excel (Microsoft Corporation, Redmond, WA), STATA 11 (StataCorp LP, College Station, TX), or Graphpad Prism (GraphPad Software, La Jolla, CA). Log transformation was performed where appropriate. Both confirmatory and exploratory analyses were performed. Two-way analysis of variance (ANOVA) was used in a confirmatory manner to test *a priori* null hypotheses that there is no heterogeneity in the percentage of neutrophils or in the amount of total protein in the recovered BALF samples caused by either treatment or mouse strain. If a significant treatment effect was detected, a one way ANOVA was performed in a post hoc exploratory manner on each mouse strain to determine which strain(s) were affected by treatment either with the saline vehicle control or the dose of QDs. If a strain showed significant differences between the treatment groups, the Tukey-Kramer (TK) method for multiple comparisons ([Kramer 1956](#)) was also used in an exploratory manner to determine which groups were indeed different from untreated controls. This is an analysis strategy modified from that used by two studies investigating both treatment and genotype effects in mice ([Berrendero et al. 2002](#); [Pittenger et al. 2006](#)). Results were considered significant if $p \leq 0.05$ with ANOVA, and if the test statistic was larger than the critical value of the TK test when $\alpha = 0.05$. In addition, linear regression was used to explore any potential associations between lung Cd and GSH

levels, and the ratio of the % neutrophils in BALF between QD treated and saline control mice.

3. Results

Animals appeared healthy prior to and during the exposure period. The range of weights in mice was quite large (~14 – 40 g) and is shown in Table 1. Lung size seemed to be proportional to bodyweight although the whole lungs were not weighed. Treatment with either a 0.9 % saline solution or QDs diluted in a 0.9% saline solution (10 nM) via oropharyngeal aspiration evoked a pulmonary inflammatory response in a mouse strain-dependent manner. This is demonstrated by a statistically significant increase in % neutrophils in BALF in some strains of mice, which can be seen in Figure 2.

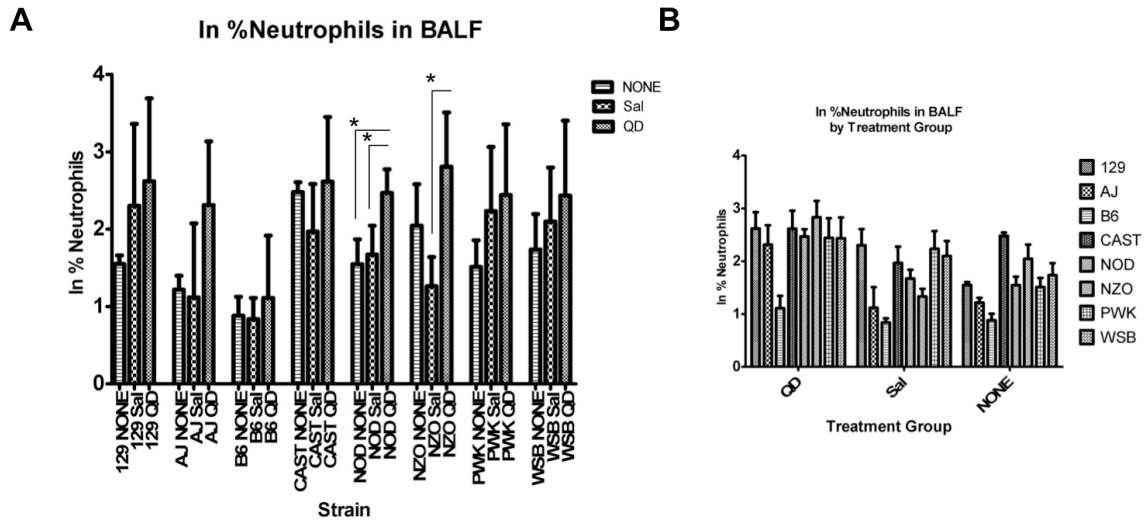


Figure 2. % Neutrophils in BALF. Plot mean \pm 95% CI of % neutrophils in BALF separated by strain (A), and by treatment group (B). Two way ANOVA found significant treatment and strain effects ($p < 0.0001$). Post hoc one-way ANOVA and the TK test found NOD/LtJ and NZO/HILtJ strains to have significant differences ($* = p < 0.05$) between treatment groups.

3.1. Neutrophils in BALF

The number of neutrophils as a percentage of total cells in the BALF is the primary biomarker of inflammation used in this study. The values were log transformed prior to analysis. The mean and 95% CI for each treatment group and strain is plotted in Figure 2 (Panels A and B). Two way ANOVA indicated significant treatment ($F_{(2,23)}=13.6$, $p<0.0001$) and strain effects ($F_{(7,23)}=7.21$, $p<0.0001$) accounting for 11.7% and 21.8% of the total variation, respectively. Post hoc one way ANOVA indicated that only specific strains, NOD/LtJ ($F_{(2,11)}=10.6$, $p=0.0027$) and NZO/HILtJ ($F_{(2,12)}=11.11$, $p=0.0019$), showed differences in % neutrophils in BALF between treatment groups. The TK test for multiple comparisons indicated that these differences were between QD and saline treated and QD and untreated groups in NOD/LtJ mice ($t_{\text{stat}}=5.33$, $t_{\text{critical}(0.05,3,11)}=3.82$), ($t_{\text{stat}}=5.81$, $t_{\text{critical}(0.05,3,11)}=3.82$), respectively. In NZO/HILtJ mice, differences in % neutrophils in BALF were found between QD treated animals and saline treated controls ($t_{\text{stat}}=6.65$, $t_{\text{critical}(0.05,3,12)}=3.77$). A/J mice also seemed to show differences across treatment groups, but they only approached statistical significance ($F_{(2,12)}=3.63.6$, $p<0.059$). Other strains did not achieve or approach statistical significance.

In Total Protein in BALF

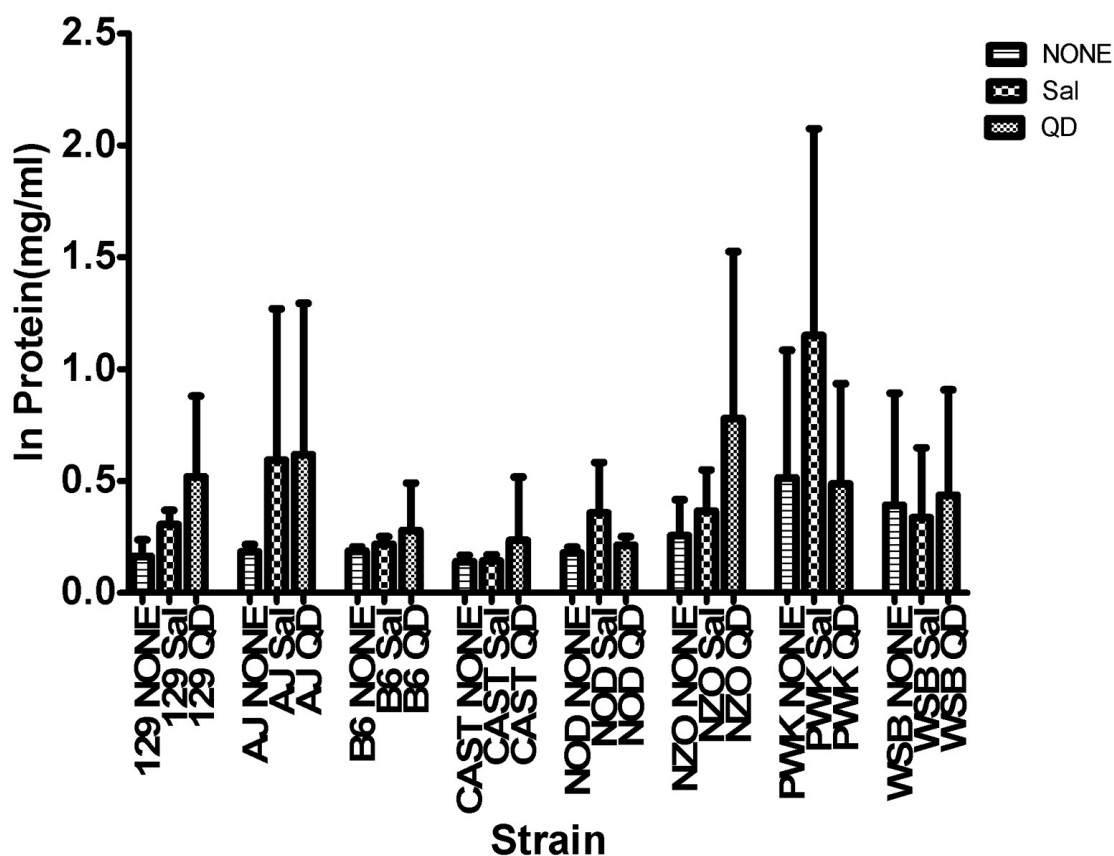


Figure 3. Total Protein in BALF. Plot of total protein in BALF shown as the mean \pm 95% CI. Two way ANOVA found significant treatment ($p=0.0471$) and strain ($p=0.0017$) effects. However, post hoc analysis revealed no differences between treatment groups in any strains.

3.2. Total protein in BALF

The amount of total protein in the BALF was chosen as a biomarker of inflammation and damage to the lung epithelium. The mean \pm 95% CI for each strain and treatment group on the linear scale can be seen in Figure 3. These data were analyzed after log transformation. Two way ANOVA indicated significant treatment ($F_{(2,23)}=3.13$, $p=0.0471$) and strain effects ($F_{(7,23)}= 3.54$, $p=0.0017$). However, post hoc analysis did not

reveal any significant differences in total protein in BALF among treatment groups within any strain.

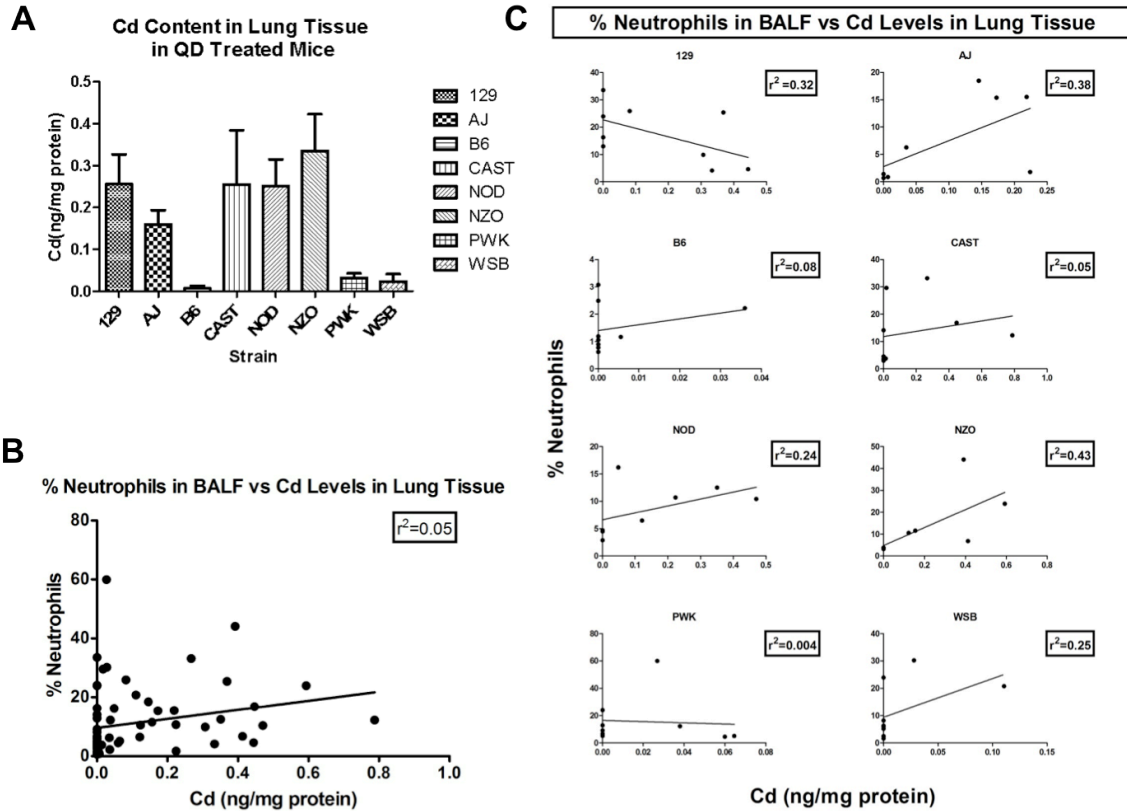


Figure 4. Cadmium Content in Lung Tissue. (A) Plot of Cd levels in right lung shown as the mean \pm SEM in QD treated animals in all strains. (B) Plot of % Neutrophils in BALF vs Cd Levels in Lung Tissue showed a weak correlation ($r^2=0.05$). (C) Plots of % Neutrophils vs. Cd Levels in Lung Tissue in individual strains showed stronger positive correlations in some strains ($r^2=0.43$ for NZO/HILtJ, $r^2=0.38$ for A/J, $r^2=0.25$ for WSB/EiJ, $r^2=0.24$ for NOD/ShiLtJ). Some strains showed weak positive correlations ($r^2=0.08$ for C57BL/6J, $r^2=0.05$ for CAST/EiJ), while others showed virtually no positive correlation ($r^2=0.004$ for PWK/PhJ) or a negative correlation ($r^2=0.32$ for an inverse correlation in 129X1/SvJ mice).

3.3. Cadmium in Lung Tissue

Cadmium in lung tissue was chosen to serve as a crude surrogate for QD exposure since Cd is a component of the semiconductor crystalline core of these nanoparticles.

Mean levels of Cd in QD treated animals from each strain is plotted in Figure 4, panel A. Since this was exploratory data analysis, no statistical tests were performed. However, there appear to be dramatic differences in Cd levels among the different mouse strains. When the mean ratio of % neutrophils between QD and saline treated groups from each strain was plotted against the lung Cd levels, a positive correlation was seen ($r^2 = 0.32$; Fig. 4B). Interestingly, the strains of mice seem to naturally split into 3 groups for Cd remaining in the lungs 8 hr after exposure.

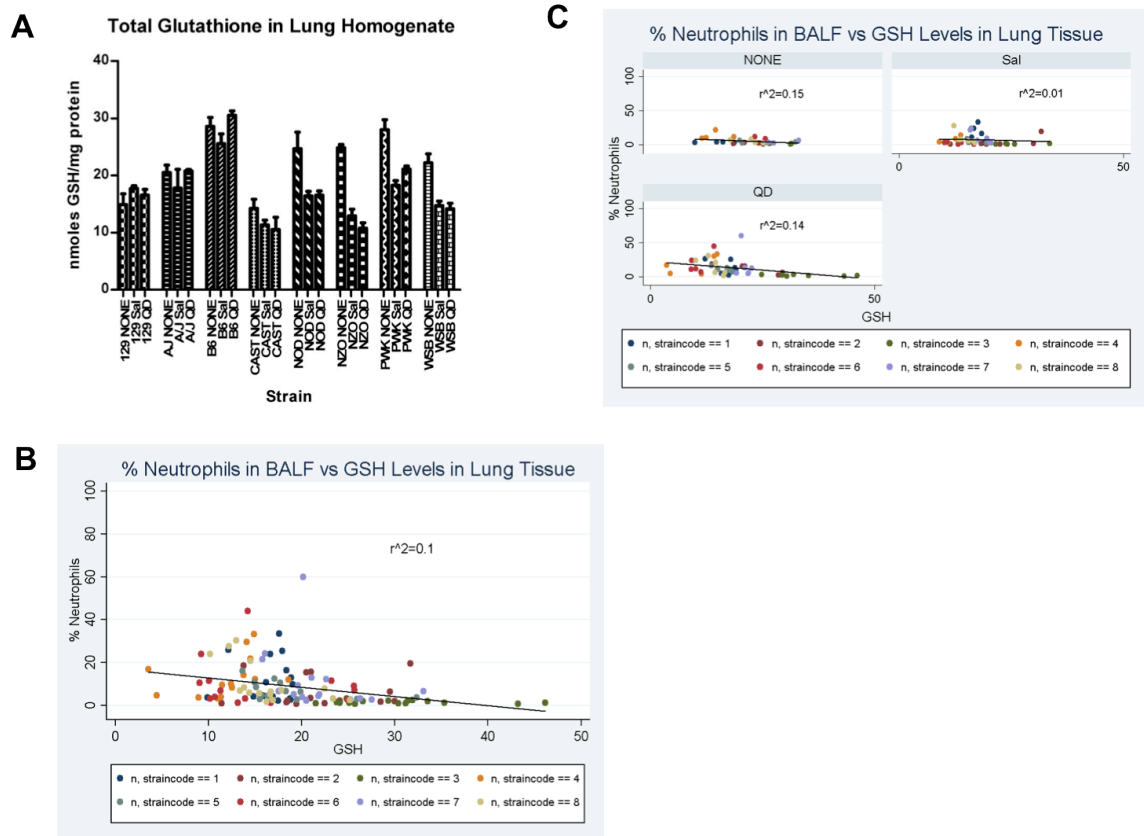


Figure 5. Total Glutathione in right lung tissue. (A) Plot of total GSH in lung tissue shown as mean \pm SEM for each strain and treatment group. Exploratory two-way ANOVA showed an interaction between treatment and strain ($p < 0.0001$ for treatment, strain, and treatment*strain). (B) Plot of %neutrophils vs GSH using all animals from all treatment groups. (C) Plots of % neutrophils against total GSH levels in lung tissue for

each treatment group. Inverse correlation can be seen on all levels but to differing degrees (untreated $r^2=0.15$, saline $r^2=0.01$, QD $r^2=0.14$).

3.4. Total GSH in Lung Tissue

Total GSH in lung tissue was chosen as a marker of oxidative stress after tissues had been collected and frozen. In an exploratory manner, a two way ANOVA of the mean levels of GSH in each strain and treatment group revealed an interaction between treatment and strain (Figure 5, panel A). The % neutrophils in BALF are plotted against GSH in lung tissue for all animals ($r^2=0.1$) in Figure 5, panel B, and by each treatment group (untreated $r^2=0.2$, saline $r^2=0.02$, QD $r^2=0.07$) in Figure 5, panel C. When the plot is split up among strains, all treatment groups have an inverse correlation but the strength varies between treatment group, which is expected given that there seems to be an interaction effect between GSH and % neutrophils.

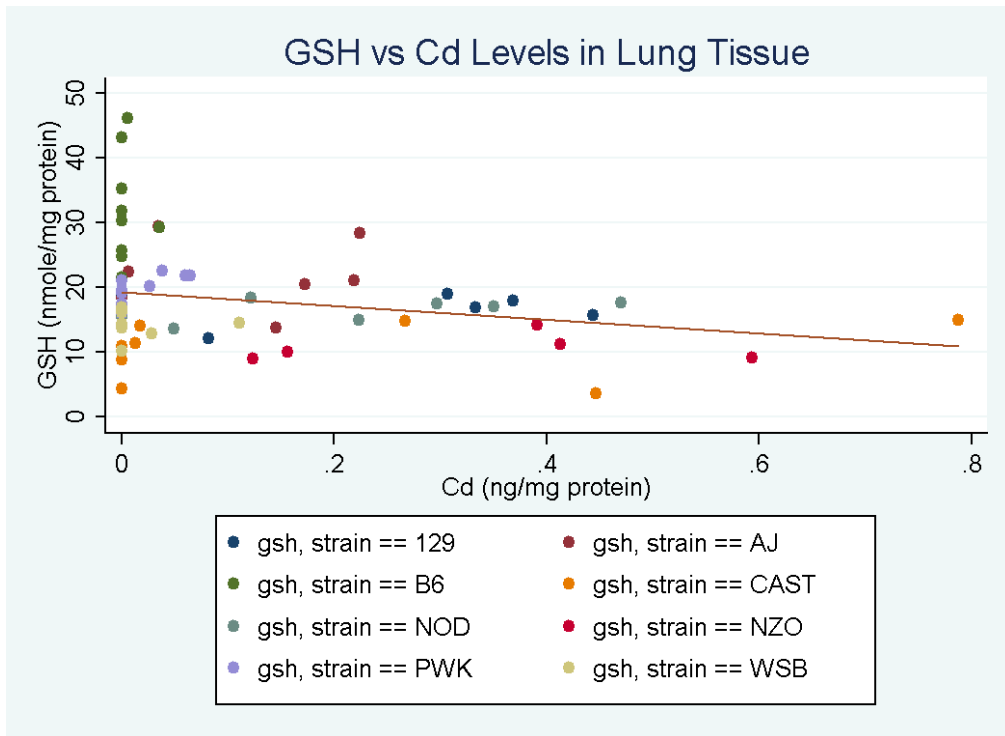


Figure 6. Correlation between Glutathione and Cadmium Levels in Lung Tissue. A plot of GSH vs Cd levels in lung tissue with the 8 mouse strains being identified by different colors. A weak inverse correlation can be observed ($r^2 = 0.06$).

3.5. Glutathione and Cadmium Correlation

When glutathione was plotted against cadmium levels, a weak inverse correlation was found. The different strains, differentiated by color in Figure 6, tend to be distributed in different ways. Some are tightly clustered on one axis such as C57BL/6J and WSB/EiJ. They both have virtually no Cd in their lung tissue. The data points for the rest of the strains are fairly widely scattered in the plot.

4. Discussion

In this study we show that exposure to QDs via oropharyngeal aspiration induces an acute inflammatory response as defined by an increase in neutrophils in BALF. However, at the current dose of 6 ug /kg BW Cd equivalent, (~15.3 pmoles QDs/kg BW) only certain strains (NOD/LtJ, NZO/HILtJ) are sensitive to this exposure. In addition, A/J mice seem to be sensitive at this dose, but due to small numbers and intra-strain variability, their response was not statistically significant. However, A/J mice do appear to be more sensitive to citrate coated Ag nanoparticles than C57BL/6J mice (Kavanagh lab, unpublished data). Graphically, C57BL/6J mice appear to be most resistant to QD induced inflammation in relation to the other strains. Two-way analysis of variance indicated that 21.8% of the variation in the primary measure of inflammatory response is due to genetic factors. This is encouraging for future studies involving a more diverse mouse population for mapping of genes that are associated with the inflammatory response induced by QD treatment.

A 2009 study examined the effects of QDs on the lung used C57 (presumably C57BL/6J) control mice and ApoE(-/-) mice on a C57 (presumably C57BL/6J) background ([Jacobsen et al. 2009](#)). The study design included two time points, 3 and 24 hr, with 2 different types of QDs (positively and negatively charged coatings) ([Jacobsen et al. 2009](#)). In that study, the authors reported that at 3 and 24 hr, controls had 6.8% and 20.6% neutrophils in BALF, respectively, and the QD treated animals had 11.1% and 93% neutrophils, respectively, with negatively charged QDs, and 10.8% and 97% neutrophils, respectively with positively charged QDs. Even at 3 hr this is high compared to the C57BL/6J mice in our study, which showed 1.47, 1.40, and 4.1% neutrophils for

the Untreated, Saline and QD treated animals, respectively, at 8 hr after exposure. However, in addition to differences in genetics (ApoE (-/-) vs. WT mice), different vehicle controls were used, the dose was ~ 1500 times higher, the particles themselves had different coatings than our particles, and the time points are different. Thus, it is not surprising to see differing degrees of inflammation in the study carried out by Jacobson et al and our study. A study using inhalation of QDs in rats ([Ma-Hock et al. 2012](#)) found 29% and 19% neutrophils in BALF at 3 and 30 days post exposure, which was over 5 days (0.52 mg Cd/m³). This study also looked at cytokines and found that several pro-inflammatory cytokines in BALF had significantly increased values in QD treated animals compared to controls at 3 days post exposure, including MDC (CCL22), MIP1- β (CCL4), MIP-2 (CXCL2), MCP-1 (CCl2), which are cytokines that will also be analyzed in the BALF samples from our current study by Pacific Northwest National Labs (PNNL). KC (CXCL1), and MIP-2 in lung tissue had increased levels in QD treated animals compared to controls at 3 days post exposure. Interestingly, at 30 days post exposure, neutrophils and all previously mentioned cytokines except MIP-2 in BALF were still increased in QD treated animals compared to controls, although to a lesser degree. MIP-2 and KC in lung tissue were increased in the QD group to the same degree. It will be interesting to compare results from our cytokine analysis when they become available with those reported by Ma-Hock et al.

Very recently, a pilot study looking at the toxicity of injected QDs was performed in Rhesus Macaques ([Ye et al. 2012](#)). In their study, little to no toxicity was noticed, and they did not find signs of an inflammatory response in terms of increases in red and white blood cells. This is more evidence that when injected, QDs do not appear to be toxic or

pro inflammatory in contrast to when they are delivered to the lungs via installation, aspiration or inhalation.

In the present study, the measurement of total protein in the BALF indicated that the dose of QDs we used does not cause physical damage to the lung, although histology should be examined to confirm this conclusion. Further examination is necessary because protein levels can increase in the lung because of increased endothelial permeability without QD induced damage to the lung epithelium ([Pittet et al. 1997](#)). While NOD/LtJ mice showed statistically significant differences between untreated and saline treated, and between untreated and QD treated, the QD and untreated levels are lower than saline indicating that there is probably some tissue damage. This is not surprising considering another study ([Jacobsen et al. 2009](#)) using tracheal installation of both (+) and (-) charged CdTe QDs in ApoE (-/-) mice found significant increases in BALF protein at 24 hr after exposure and with a dose approximately 1500 times higher in terms of Cd equivalency than the dose in our study. But this estimate would vary since our mouse body weights varied from ~14 g to ~40 g, and the ApoE (-/-) mice are on a C57 (presumably C57BL/6J) background and C57 controls are roughly in the middle of that BW spectrum. Cadmium levels in the lung tissue were not analyzed independently for differences between strains but graphically they appear to be different and are weakly correlated over all with the mean % neutrophils of each strain, but more strongly correlated in some strains ($r^2=0.43$ for NZO, $r^2=0.38$ for AJ). This is an important observation since QDs can release Cd ions ([Derfus et al. 2004](#); [Kirchner et al. 2005](#); [Su et al. 2010](#)), Cd can cause oxidative stress ([Watanabe et al. 2003](#)) via generating ROS by disrupting the electron transport chain ([Wang et al. 2004](#)), and the generation of ROS and oxidative

stress are implicated as mechanisms of QD toxicity ([Lovrić et al. 2005](#); [Clift et al. 2010](#)). A caveat to this interpretation is that the method we used to measure Cd (ICP-MS) did not distinguish between free Cd released *in vivo* from intact QDs in the tissues after acid digestion of the samples. One method that could be employed in the future to potentially help distinguish between free Cd and QD bound Cd would be to measure metallothionein (MT) mRNA in lung tissue, which is inducible by free Cd ([Vašák and Hasler 2000](#)). If MT was upregulated in lung tissue of QD treated animals it would be an indication of the presence of free Cd. However, the MT1/2 gene in mice is known to also harbor the AP-1 ([Davis and Cousins 2000](#)) regulatory element, which could be activated by the inflammatory response. Alternatively, separation of QDs by ultracentrifugation from free/protein bound Cd in tissue homogenates may provide another possible technique to resolve this issue.

Other *in vivo* studies which have looked at Cd in tissue after exposure to QDs, albeit by injection, found that after 1 day, the major deposits of Cd are in the kidney, liver and spleen ([Hauck et al. 2010](#); [Su et al. 2011](#); [Ye et al. 2012](#)). When measured at 8 hr, Su et al. found the lung to be a large repository of Cd as well. Interestingly, when QDs were delivered via nasal installation, the lungs were the only organ found to contain significant Cd (Kavanagh Lab, unpublished data). In addition, it was found that when QDs are inhaled, Cd levels decrease in the lung, and increase in the liver and kidney over time (between day and 26 post exposure) ([Ma-Hock et al. 2012](#)).

Glutathione (GSH) is an important intracellular antioxidant and in this study we measured total glutathione (GSH + GSSG) in the lung tissue as a biomarker of oxidative stress since depletion of GSH is a sign of oxidative stress. We observed an interaction

between treatment and strain in relation to GSH levels indicating that any potential relationship between GSH levels and strain is dependent on treatment. This dependency can be visualized when the correlation observed between GSH levels and the % neutrophils are categorized by treatment and plotted as in Figure 5, panel C. Even though the strains have different distributions on the correlation plots (depending on treatment group), there is an overall weak inverse correlation. The analysis of variance suggests that some of the inflammation phenotype measured by neutrophils in BALF is related to GSH content. Interestingly, C57BL/6J (one of the strains of mice that appear to be the most resistant to inflammation) had the highest levels of GSH. While total glutathione is not as good a measure of oxidative stress as the ratio of reduced to oxidized glutathione (GSH/GSSG) which has been used in numerous studies, measuring the GSH/GSSG ratio requires homogenizing the tissue and mixing the homogenate 1:1 with 10% 5-sulfosalicylic acid (SSA) at the time of necropsy to avoid oxidation of GSH to GSSG during storage. Our primary focus on the necropsy day was collecting and processing the cellular fraction of the BALF for Cytospin cartridge preparation and immunohistochemical staining for flow cytometry. As a result tissues were frozen immediately and total glutathione was measured in the right lung at a later date. Interestingly, one study that measured both GSH and GSSG as a biomarker of QD induced oxidative stress ended up only reporting and using GSH levels in their assessment because GSSG levels were below the limit of detection ([Clift et al. 2010](#)). Their inability to measure GSSG could be interpreted as evidence that only a mild but significant oxidative stress is occurring with QD treatment in their dose range of 0 to 80 nM QDs. If this is true it is likely the case that any oxidative stress occurring in the lung

tissue is too mild to cause detectable depletion of glutathione between saline and QD treatment animals which would be the most direct indication of QDs effect on oxidative stress. However we cannot be sure because this analysis was done in an exploratory manner. In future studies, the lung tissue should be divided immediately after necropsy and stored properly to avoid oxidation of GSH to GSSG so that the ratio may be measured.

Since Cd released from QDs is thought to cause oxidative stress, and GSH is used as a biomarker for oxidative stress, we determined if there was any correlation between these measures. The weak correlation found suggests that GSH levels are slightly reduced with increasing levels of Cd (Figure 6). This could be interpreted as a sign of mild oxidative stress occurring from the increased presence of Cd, perhaps from either increased degradation of QDs or decreased clearance of Cd in the lungs. However, confirmatory studies using additional measures of oxidative stress such as measuring the GSH/GSSG ratio, measuring malondialdehyde (MDA) in plasma, 3-nitrotyrosine immunostaining, or using agents such as 5,5-dimethyl-1-pyrroline N-oxide (DMPO) ([Halliwell and Whiteman 2004](#)) to trap free radical species in lung tissue need to be performed to confirm that oxidative stress is happening.

In conclusion, we have shown that QDs induce mild lung inflammation when delivered via OPA at a dose of 6 ug Cd equivalent/kg BW in an *in vivo* multiple strain mouse model. However, the inflammatory response is strain dependent and only certain strains show significant increases in inflammatory biomarkers. The differential responses among these 8 strains was an important finding in that another study to map genes associated with QD inflammation susceptibility is being planned using either RI strains,

the Diversity Outbred Cross (which is a set derived ultimately from the 8 strains that were used in this study), or the AxB, BxA cross strains. In addition, our exploratory data suggest that the mechanisms of QD toxicity that other studies have postulated, including the release of free Cd, depletion of GSH, and subsequent oxidative stress, could be contributing to the observed inflammatory response.

References

- Berrendero, F., B. L. Kieffer and R. Maldonado (2002). "Attenuation of Nicotine-Induced Antinociception, Rewarding Effects, and Dependence in {micro}-Opioid Receptor Knock-Out Mice." J. Neurosci. 22: 10935-10940.
- Chakravarthy, K. V., B. A. Davidson, J. D. Helinski, H. Ding, W.-C. Law, K.-T. Yong, . . . P. R. Knight (2011). "Doxorubicin-conjugated quantum dots to target alveolar macrophages and inflammation." Nanomedicine: Nanotechnology, Biology and Medicine 7: 88-96.
- Chen, F. and D. Gerion (2004). "Fluorescent CdSe / ZnS Nanocrystal – Peptide Conjugates for Long-term , Nontoxic Imaging and Nuclear Targeting in Living Cells." Nano.
- Churchill, G. a., D. C. Airey, H. Allayee, J. M. Angel, A. D. Attie, J. Beatty, . . . F. Zou (2004). "The Collaborative Cross, a community resource for the genetic analysis of complex traits." Nature genetics 36: 1133-1137.
- Clift, M. J., M. S. Boyles, D. M. Brown and V. Stone (2010). "An investigation into the potential for different surface-coated quantum dots to cause oxidative stress and affect macrophage cell signalling in vitro." Nanotoxicology 4(2): 139-149.
- Clift, M. J. D., C. Brandenberger, B. Rothen-Rutishauser, D. M. Brown and V. Stone (2011). "The uptake and intracellular fate of a series of different surface coated quantum dots in vitro." Toxicology 286(1-3): 58-68.
- Davis, S. R. and R. J. Cousins (2000). "Metallothionein Expression in Animals: A Physiological Perspective on Function." The Journal of Nutrition 130(5): 1085-1088.
- Derfus, A. M., W. C. W. Chan and S. N. Bhatia (2004). "Probing the Cytotoxicity of Semiconductor Quantum Dots." Nano Letters 4: 11-18.
- EPA, U. (2007). METHOD 6020A INDUCTIVELY COUPLED PLASMA-MASS SPECTROMETRY.
- Geys, J., A. Nemmar, E. Verbeken, E. Smolders, M. Ratoi, M. F. Hoylaerts, . . . P. H. M. Hoet (2008). "Acute Toxicity and Prothrombotic Effects of Quantum Dots: Impact of Surface Charge." Environ Health Perspect 116(12).
- Halliwell, B. and M. Whiteman (2004). "Measuring reactive species and oxidative damage in vivo and in cell culture: how should you do it and what do the results mean?" British Journal of Pharmacology 142(2): 231-255.
- Hauck, T. S., R. E. Anderson, H. C. Fischer, S. Newbigging and W. C. Chan (2010). "In vivo quantum-dot toxicity assessment." Small 6(1): 138-144.
- Hoshino, A., K. Fujioka, T. Oku, M. Suga, Y. F. Sasaki, T. Ohta, . . . K. Yamamoto (2004). "Physicochemical Properties and Cellular Toxicity of Nanocrystal Quantum Dots Depend on Their Surface Modification." Nano Letters 4: 2163 <last_page> 2169.
- Hoshino, A., S. Hanada, N. Manabe, T. Nakayama and K. Yamamoto (2009). "Immune response induced by fluorescent nanocrystal quantum dots in vitro and in vivo." NanoBioscience, IEEE Transactions on 8: 51-57.
- Hoshino, A., S. Hanada and K. Yamamoto (2011). "Toxicity of nanocrystal quantum dots: the relevance of surface modifications." Archives of toxicology 85: 707-720.
- Iavicoli, I., E. J. Calabrese and M. A. Nascarella (2010). "Exposure to nanoparticles and hormesis." Dose Response 8(4): 501-517.
- Jacobsen, N. R., P. Moller, K. A. Jensen, U. Vogel, O. Ladefoged, S. Loft and H. Wallin (2009). "Lung inflammation and genotoxicity following pulmonary exposure to nanoparticles in ApoE-/- mice." Part Fibre Toxicol 6: 2.
- Kelada, S. N. P., D. L. Aylor, B. C. E. Peck, J. F. Ryan, U. Tavaréz, R. J. Buus, . . . F. S. Collins (2012). "Genetic Analysis of Hematological Parameters in Incipient Lines of the Collaborative Cross." G3: Genes|Genomes|Genetics 2(2): 157-165.
- Kim, S., Y. T. Lim, E. G. Soltesz, A. M. De Grand, J. Lee, A. Nakayama, . . . J. V. Frangioni (2004). "Near-infrared fluorescent type II quantum dots for sentinel lymph node mapping." Nat Biotechnol 22(1): 93-97.
- Kirchner, C., T. Liedl, S. Kudera, T. Pellegrino, A. Muñoz Javier, H. E. Gaub, . . . W. J. Parak (2005). "Cytotoxicity of colloidal CdSe and CdSe/ZnS nanoparticles." Nano letters 5: 331-338.
- Kramer, C. Y. (1956). "Extension of Multiple Range Tests to Group Means with Unequal Numbers of Replications." Biometrics 12(3): 307-310.
- Lovric, J., H. S. Bazzi, Y. Cuie, G. R. Fortin, F. M. Winnik and D. Maysinger (2005). "Differences in subcellular distribution and toxicity of green and red emitting CdTe quantum dots." J Mol Med (Berl) 83(5): 377-385.
- Lovrić, J., S. J. Cho, F. M. Winnik and D. Maysinger (2005). "Unmodified Cadmium Telluride Quantum Dots Induce Reactive Oxygen Species Formation Leading to Multiple Organelle Damage and Cell Death." Chemistry & biology 12: 1227-1234.

- Ma-Hock, L., S. Brill, W. Wohlleben, P. M. A. Farias, C. R. Chaves, D. P. L. A. Tenório, . . . B. van Ravenzwaay (2012). "Short term inhalation toxicity of a liquid aerosol of CdS/Cd(OH)₂ core shell quantum dots in male Wistar rats." Toxicology Letters 208(2): 115-124.
- McConnachie, L. A., C. C. White, D. Botta, M. E. Zadworny, D. P. Cox, R. P. Beyer, . . . T. J. Kavanagh (2012). "Heme oxygenase expression as a biomarker of exposure to amphiphilic polymer-coated CdSe/ZnS quantum dots." Nanotoxicology: 1-11.
- Medintz, I. L., H. T. Uyeda, E. R. Goldman and H. Mattoussi (2005). "Quantum dot bioconjugates for imaging, labelling and sensing." Nat Mater 4: 435-446.
- Nadeau, J. H. and A. M. Dudley (2011). "Genetics. Systems genetics." Science (New York, N.Y.) 331: 1015-1016.
- Pittenger, C., S. Fasano, D. Mazzocchi-Jones, S. B. Dunnett, E. R. Kandel and R. Brambilla (2006). "Impaired bidirectional synaptic plasticity and procedural memory formation in striatum-specific cAMP response element-binding protein-deficient mice." The Journal of neuroscience : the official journal of the Society for Neuroscience 26: 2808-2813.
- Pittet, J. F., R. C. Mackersie, T. R. Martin and M. A. Matthay (1997). "Biological markers of acute lung injury: prognostic and pathogenetic significance." American Journal of Respiratory and Critical Care Medicine 155(4): 1187-1205.
- Savla, R., O. Taratula, O. Garbuzenko and T. Minko (2011). "Tumor targeted quantum dot-mucin 1 aptamer-doxorubicin conjugate for imaging and treatment of cancer." Journal of controlled release : official journal of the Controlled Release Society 153: 16-22.
- Shiohara, A., A. Hoshino, K. Hanaki, K. Suzuki and K. Yamamoto (2004). "On the cyto-toxicity caused by quantum dots." Microbiology and Immunology 48: 669-675.
- Su, Y., M. Hu, C. Fan, Y. He, Q. Li, W. Li, . . . Q. Huang (2010). "The cytotoxicity of CdTe quantum dots and the relative contributions from released cadmium ions and nanoparticle properties." Biomaterials 31: 4829-4834.
- Su, Y., F. Peng, Z. Jiang, Y. Zhong, Y. Lu, X. Jiang, . . . Y. He (2011). "In vivo distribution, pharmacokinetics, and toxicity of aqueous synthesized cadmium-containing quantum dots." Biomaterials 32(25): 5855-5862.
- Vašák, M. and D. W. Hasler (2000). "Metallothioneins: new functional and structural insights." Current Opinion in Chemical Biology 4(2): 177-183.
- Wang, Y., J. Fang, S. S. Leonard and K. M. Krishna Rao (2004). "Cadmium inhibits the electron transfer chain and induces Reactive Oxygen Species." Free Radical Biology and Medicine 36(11): 1434-1443.
- Watanabe, M., K. Henmi, K. i. Ogawa and T. Suzuki (2003). "Cadmium-dependent generation of reactive oxygen species and mitochondrial DNA breaks in photosynthetic and non-photosynthetic strains of *Euglena gracilis*." Comparative Biochemistry and Physiology Part C: Toxicology & Pharmacology 134(2): 227-234.
- Weldy, C. S., C. C. White, H.-W. Wilkerson, T. V. Larson, J. A. Stewart, S. E. Gill, . . . T. J. Kavanagh (2011). "Heterozygosity in the glutathione synthesis gene *Gclm* increases sensitivity to diesel exhaust particulate induced lung inflammation in mice." Inhalation Toxicology 23(12): 724-735.
- Wu, X., H. Liu, J. Liu, K. N. Haley, J. A. Treadway, J. P. Larson, . . . M. P. Bruchez (2003). "Immunofluorescent labeling of cancer marker Her2 and other cellular targets with semiconductor quantum dots." Nat Biotechnol 21(1): 41-46.
- Yazdi, A. S., G. Guarda, N. Riteau, S. K. Drexler, A. Tardivel, I. Couillin and J. Tschopp (2010). "Nanoparticles activate the NLR pyrin domain containing 3 (Nlrp3) inflammasome and cause pulmonary inflammation through release of IL-1 α and IL-1 β ." Proceedings of the National Academy of Sciences of the United States of America 107: 19449-19454.
- Ye, L., K.-T. Yong, L. Liu, I. Roy, R. Hu, J. Zhu, . . . P. N. Prasad (2012). "A pilot study in non-human primates shows no adverse response to intravenous injection of quantum dots." Nat Nano advance online publication.
- Zhang, L. W., W. W. Yu, V. L. Colvin and N. A. Monteiro-Riviere (2008). "Biological interactions of quantum dot nanoparticles in skin and in human epidermal keratinocytes." Toxicology and applied pharmacology 228: 200-211.